PS3

Assignment 03 Report

Name: XU JUNPENG (许俊鹏)　**SID:** 12532726

1. Global Methane Levels from 2003–2020

1.1 Monthly Climatology of Methane

Method

1. Loaded the C3S merged greenhouse-gas product `200301_202006-C3S-L3_GHG-PRODUCTS-OBS4MIPS-MERGED-v4.3.nc`, and used the variable xch4 (column-averaged CH_4 in ppb) on a 5°×5° lat–lon grid from 2003-01 to 2020-06.
2. Converted the time coordinate to a `DatetimeIndex` and extracted month numbers (1–12) for each time step.
3. Treated unrealistically large values (>1×10^{20}) as missing and replaced them with NaN so they do not affect averages.
4. For each calendar month m = 1-12, selected all time steps whose month equals m and computed the mean over time at every grid cell.
5. Arranged the resulting 12 two-dimensional fields into a 12-panel figure, each panel showing one month’s climatological distribution.

Results

- The 12 panels show a clear seasonal migration of high methane regions.
- Enhanced CH_4 appears over the Northern Hemisphere during boreal late autumn–winter, consistent with strong anthropogenic emissions and weaker OH removal.
- During boreal summer, the Northern Hemisphere values decrease slightly while tropical regions remain relatively high, reflecting persistent tropical emissions and efficient vertical mixing.
- The Southern Hemisphere exhibits weaker seasonality and lower overall concentrations, with modest enhancements over South America and southern Africa during their biomass burning seasons.

- Overall, the climatology confirms that both emissions and seasonal chemistry control the global distribution, with strongest column methane over densely populated and wetland/biomass-burning regions.

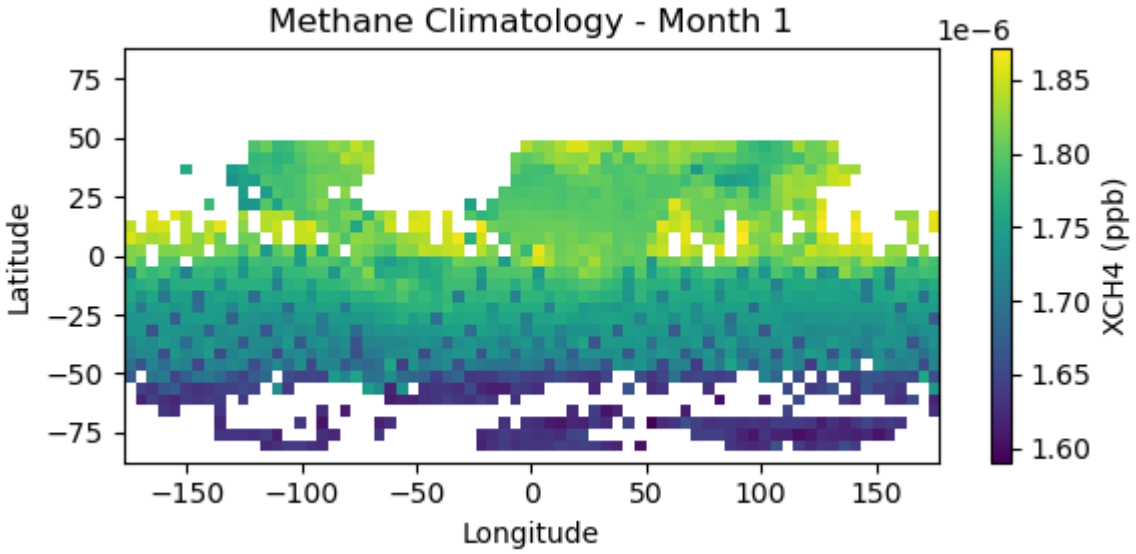

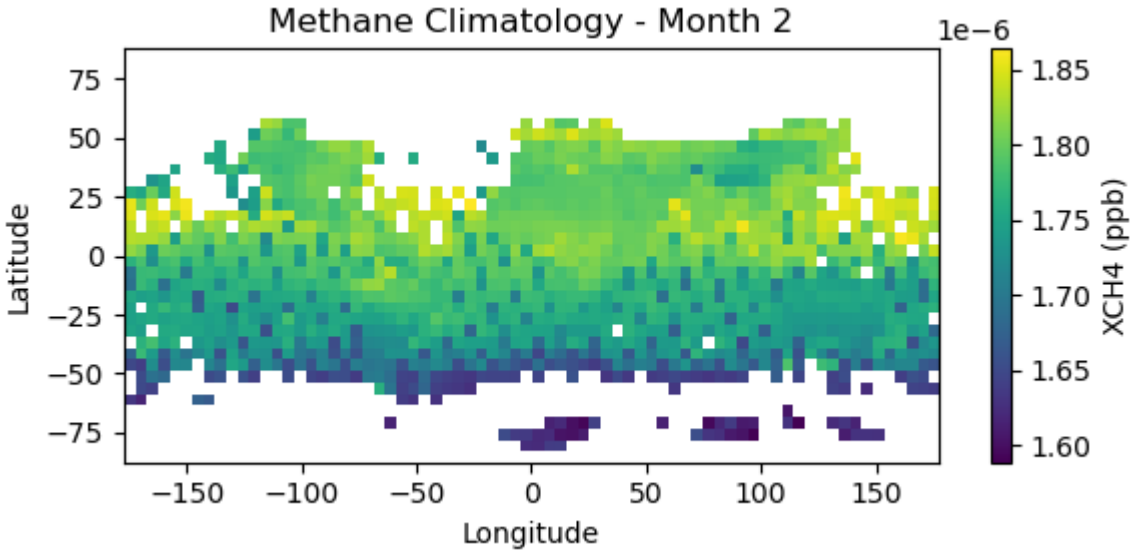

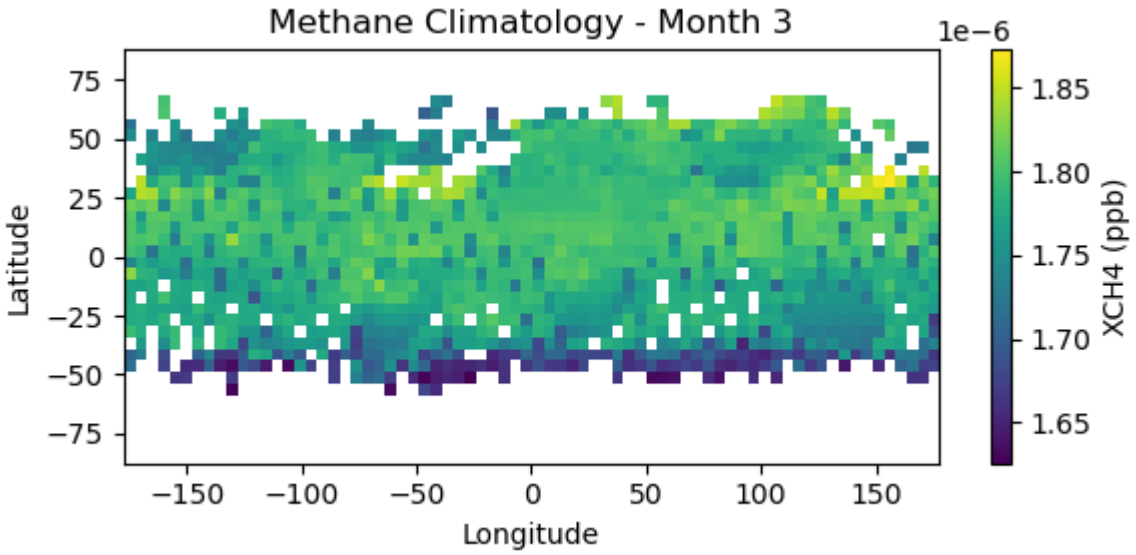
Methane Climatology - Month 3
1e−6
1.85
1.80
1.75
1.70
1.65
XCH4 (ppb)
Latitude
75
50
25
0
−25
−50
−75
−150
−100
−50
0
50
100
150
Longitude

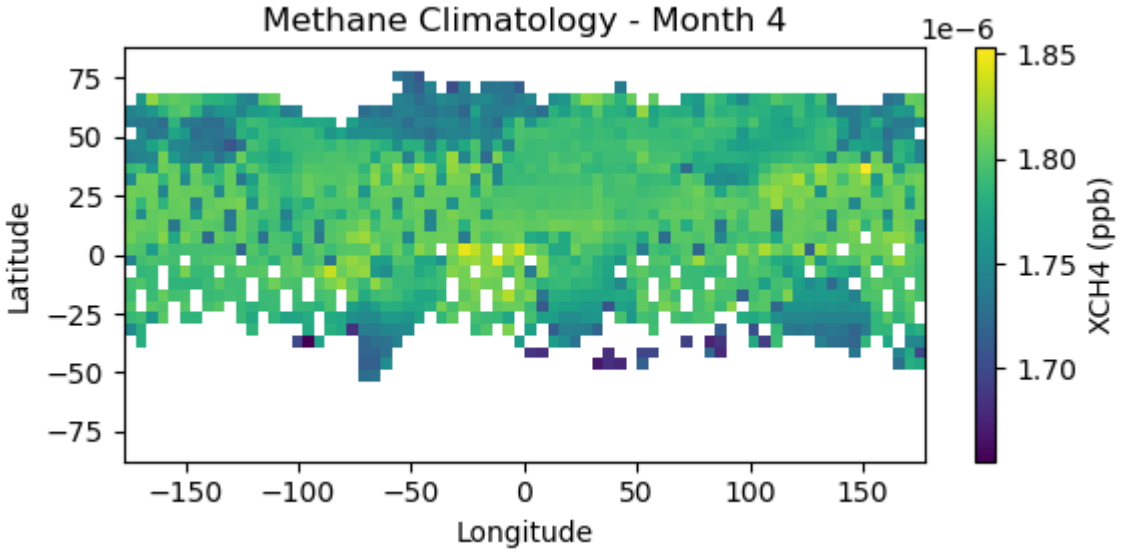
Methane Climatology - Month 4
1e−6
1.85
1.80
1.75
1.70
XCH4 (ppb)
Latitude
75
50
25
0
−25
−50
−75
−150
−100
−50
0
50
100
150
Longitude

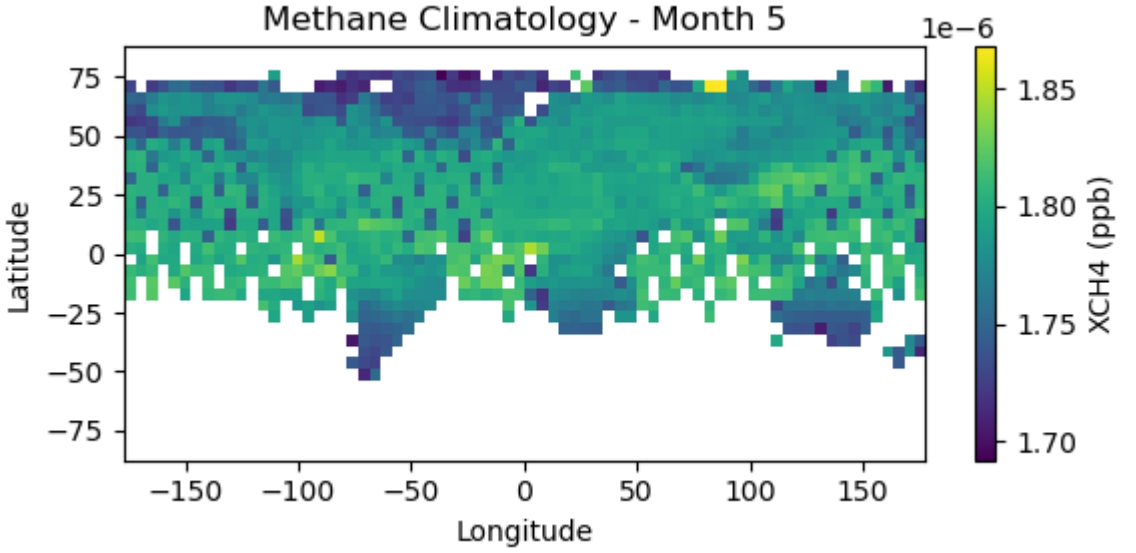
Methane Climatology - Month 5
1e−6
1.85
1.80
1.75
1.70
XCH4 (ppb)
Latitude
75
50
25
0
−25
−50
−75
−150
−100
−50
0
50
100
150
Longitude

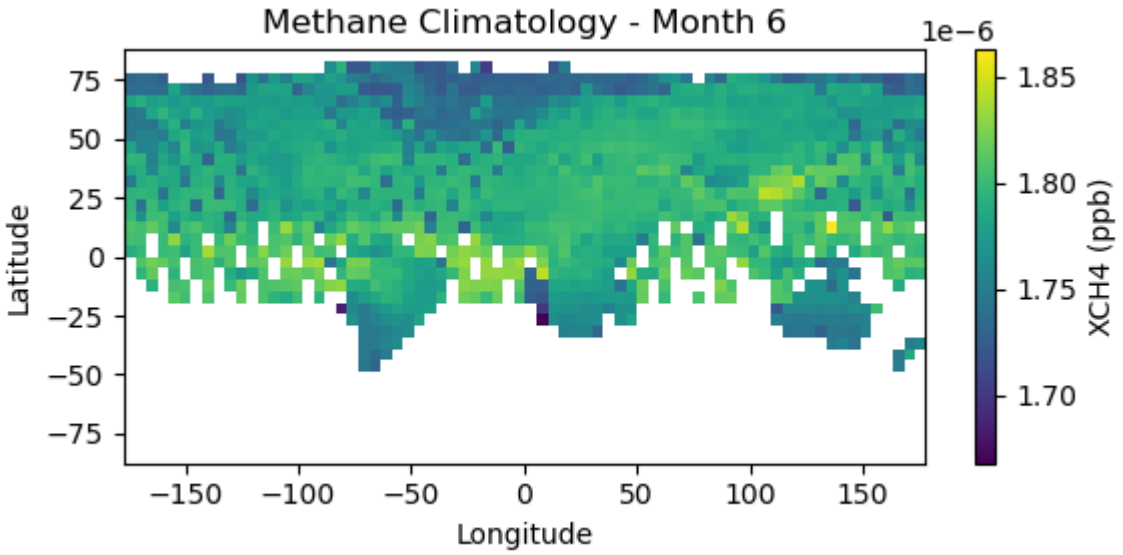
Methane Climatology - Month 6
1e−6
1.85
1.80
1.75
1.70
XCH4 (ppb)
Latitude
75
50
25
0
−25
−50
−75
−150
−100
−50
0
50
100
150
Longitude

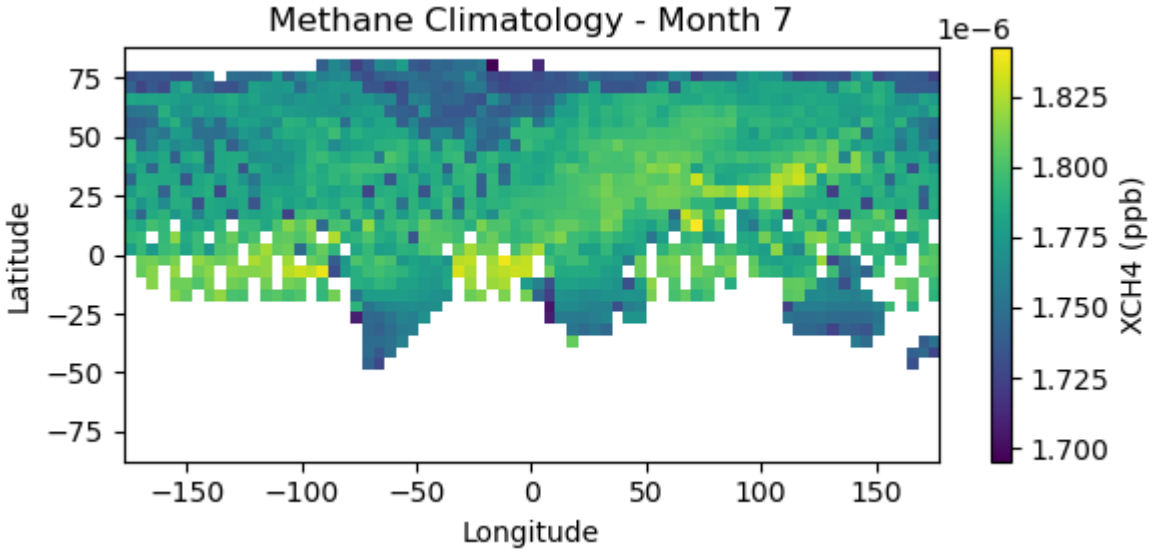
Methane Climatology - Month 7
1e−6
1.825
1.800
1.775
1.750
1.725
1.700
XCH4 (ppb)
Latitude
75
50
25
0
−25
−50
−75
−150
−100
−50
0
50
100
150
Longitude

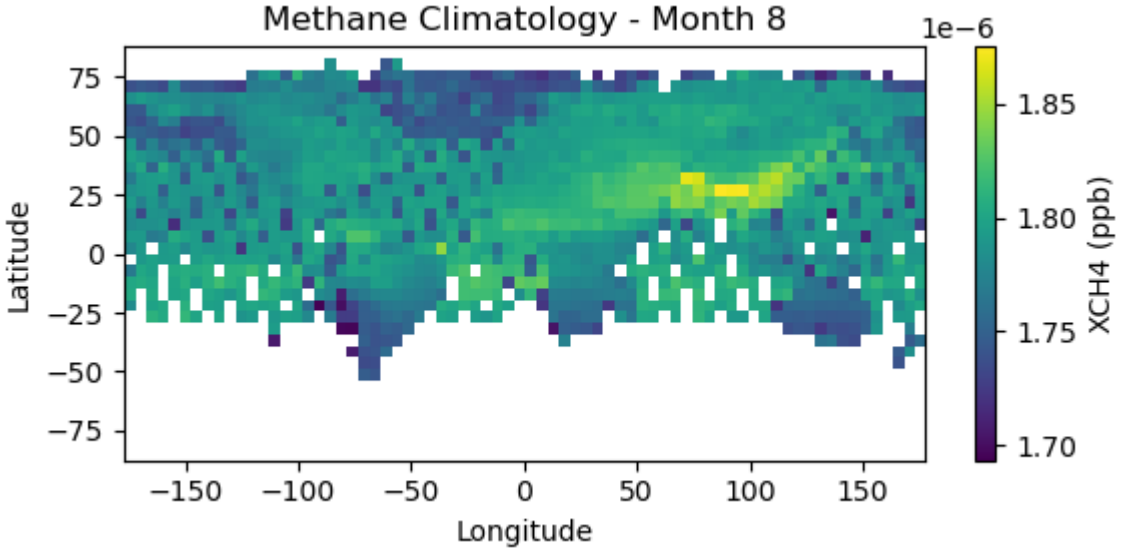
Methane Climatology - Month 8
1e−6
1.85
1.80
1.75
1.70
XCH4 (ppb)
Latitude
75
50
25
0
−25
−50
−75
−150
−100
−50
0
50
100
150
Longitude

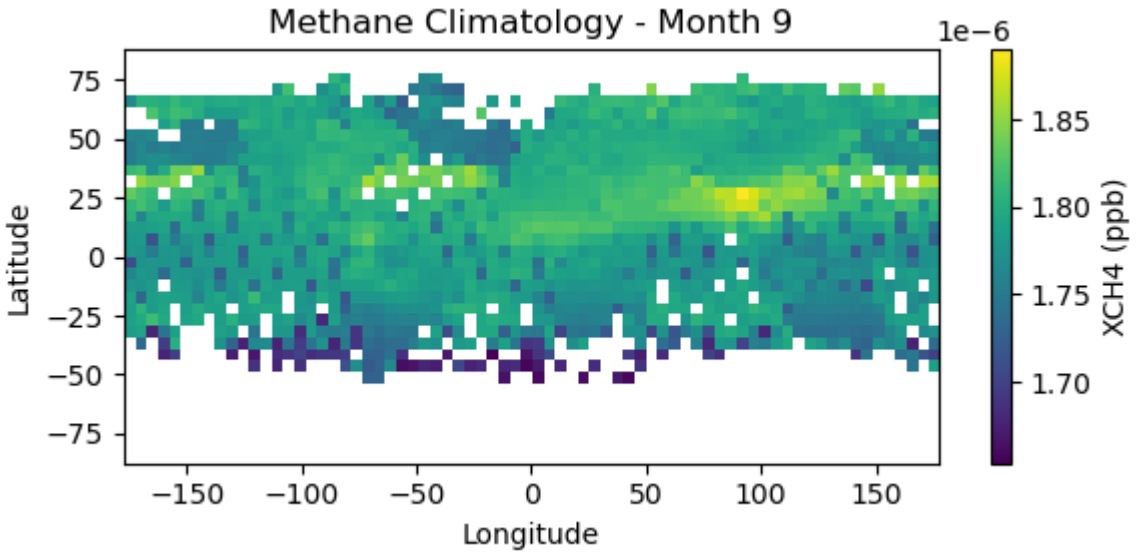
Methane Climatology - Month 9
1e−6
1.85
1.80
1.75
1.70
XCH4 (ppb)
75
50
25
0
−25
−50
−75
Latitude
−150
−100
−50
0
50
100
150
Longitude

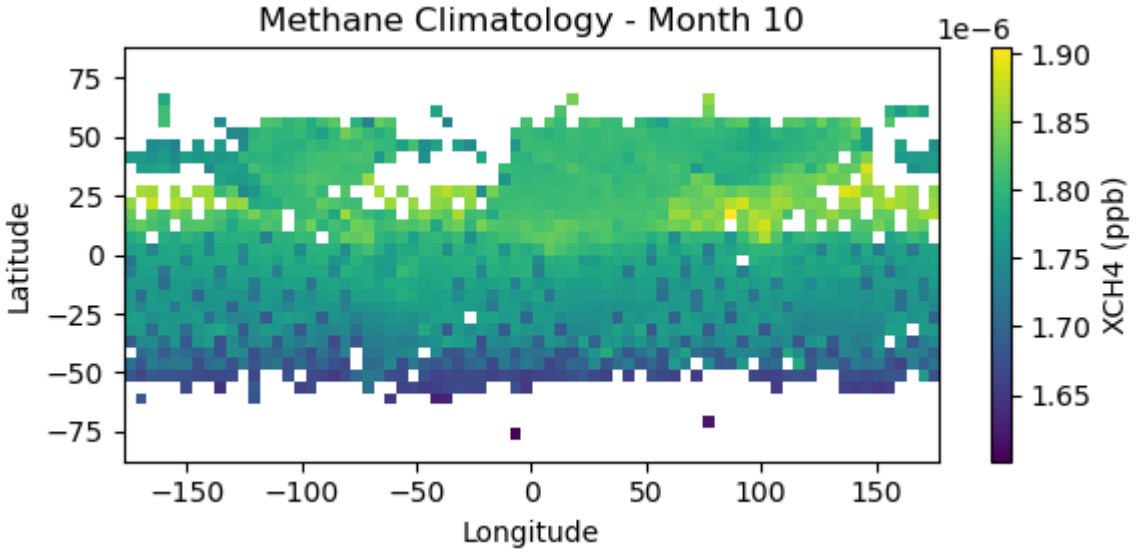
Methane Climatology - Month 10
1e−6
1.90
1.85
1.80
1.75
1.70
1.65
XCH4 (ppb)
75
50
25
0
−25
−50
−75
Latitude
−150
−100
−50
0
50
100
150
Longitude

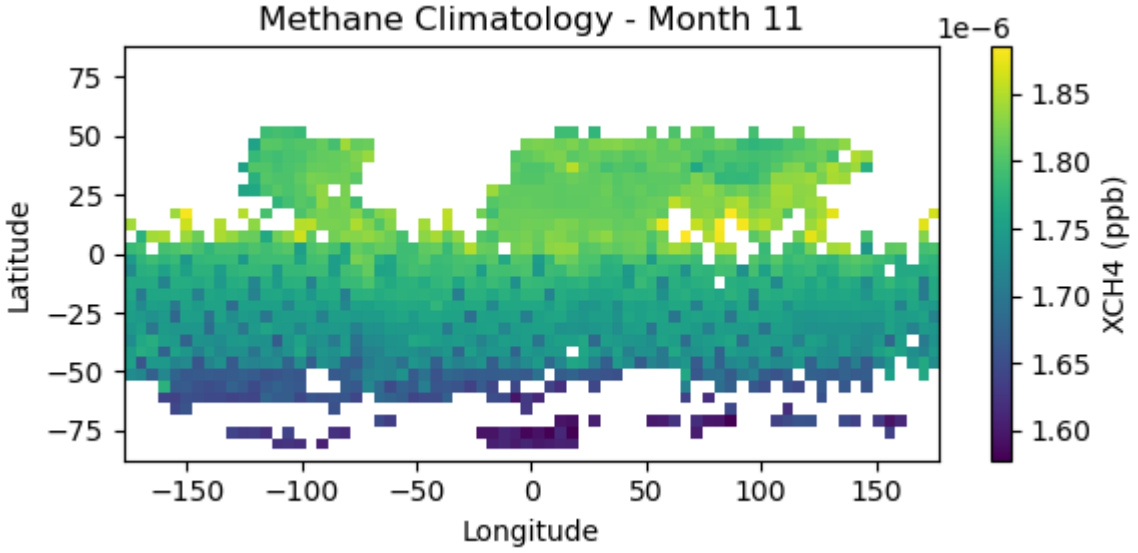
Methane Climatology - Month 11
1e−6
1.85
1.80
1.75
1.70
1.65
1.60
XCH4 (ppb)
75
50
25
0
−25
−50
−75
Latitude
−150
−100
−50
0
50
100
150
Longitude

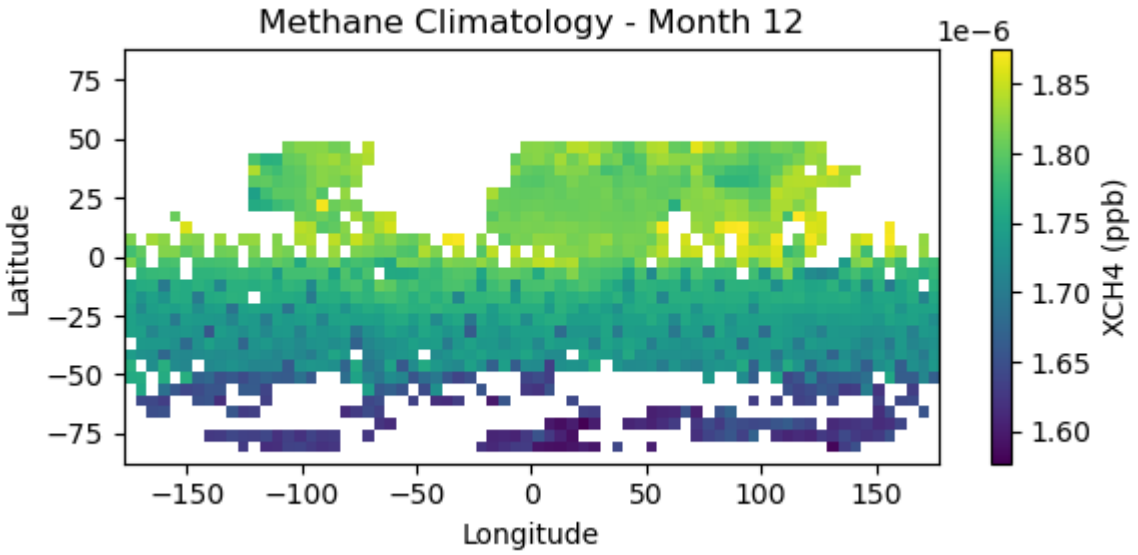

1.2 Globally averaged methane time series

Method

1. Used the same xch4 field and converted the time coordinate to monthly timestamps.
2. Applied an area weighting proportional to cos(latitude) to account for the shrinking area of high-latitude grid cells.
3. For each month, computed a weighted mean over all valid grid cells to obtain a global mean column CH_4 time series.
4. Plotted the resulting series from 2003-01 to 2020-06 and visually compared it with the reference plot provided in the assignment.

Results

- The global mean methane series shows:
  - A pronounced overall upward trend throughout 2003–2020, reflecting continued growth in global methane burden.
  - A superimposed regular annual cycle with amplitude of roughly a few tens of ppb.
  - Year-to-year variability in the seasonal peaks and troughs, indicating interannual changes in emissions and sinks (e.g., wetland anomalies, OH variability, fires).
- The timing and magnitude of peaks and valleys qualitatively match the reference figure: methane generally peaks near late boreal winter/early spring and reaches minima in boreal summer when OH sink is strongest.
- The steady rise, combined with modest interannual fluctuations, is consistent with the known resumption of methane growth after the early-2000s plateau.

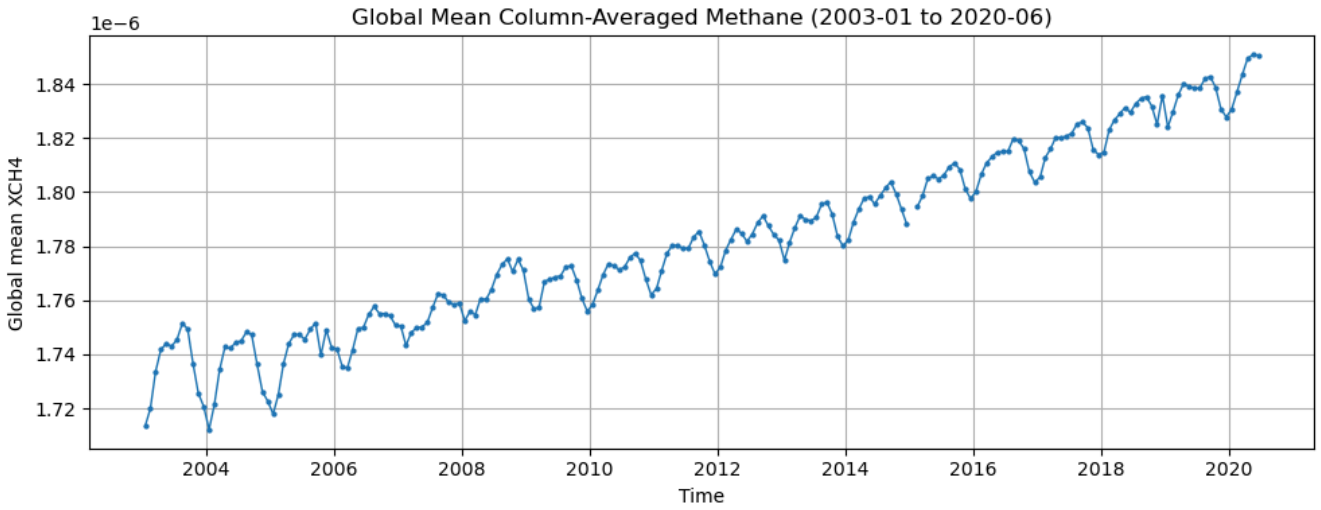

1.3 Deseasonalized methane at [15°S, 150°W]

Method

1. Chose the target location (15°S, 150°W). Located the closest model grid cell by minimizing the absolute difference in latitude and longitude.
2. Extracted the full time series of xch4 at that single grid cell from 2003-01 to 2020-06.
3. Computed a local monthly climatology: for each calendar month (Jan–Dec), averaged all values belonging to that month at this grid point.
4. Subtracted the corresponding monthly climatology value from each observation to obtain a deseasonalized anomaly series.
5. Plotted the anomaly time series to highlight interannual variability and long-term changes, with a horizontal zero line for reference.

Results

- Before deseasonalization, the point series exhibits a clear annual cycle similar to the global mean, plus a gentle long-term increase.
- After subtracting the monthly climatology, the annual cycle is largely removed and the series fluctuates around zero with a slowly rising background:
  - Anomalies typically lie within about ±(a few ×10 ppb), indicating that local year-to-year variability is modest relative to the mean level.
  - Several multiyear periods display predominantly positive anomalies, especially in the later years of the record, consistent with the global growth in methane.
  - Short negative excursions correspond to years when local CH_4 at this location is slightly below its climatological value, possibly linked to circulation changes or

regional sink variations.

- Overall, the deseasonalized series emphasizes interannual variability and the underlying long-term increase at this South Pacific location once the regular seasonal cycle is removed.

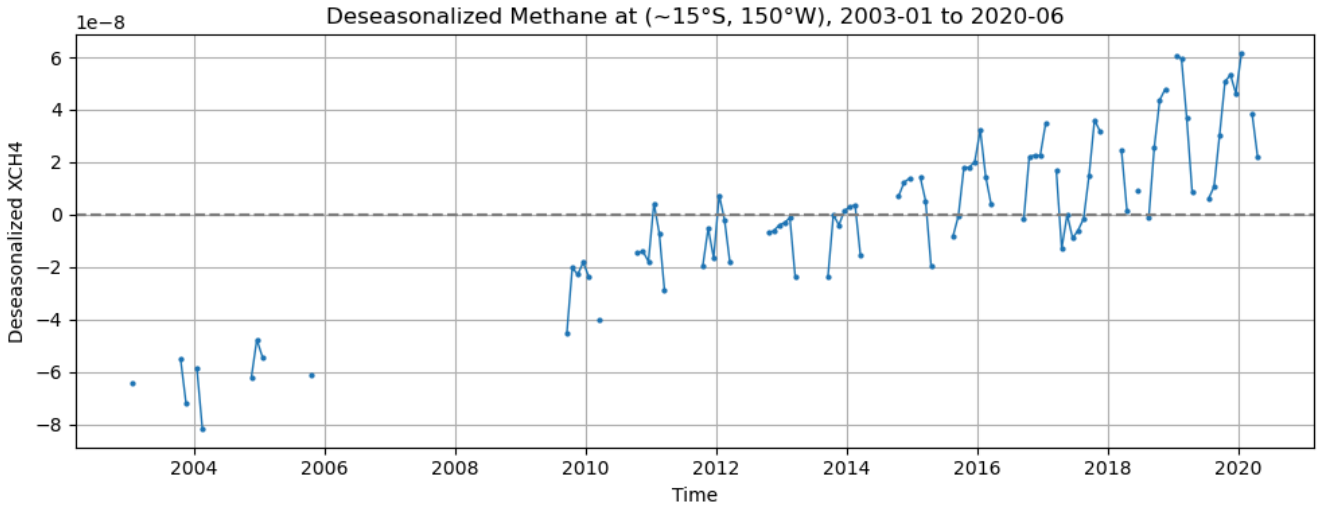

2. Niño 3.4 index from NOAA ERSST

2.1 Monthly climatology and anomalies in Niño 3.4 region

Method

1. Opened the NOAA ERSST v3b sea surface temperature dataset `NOAA_NCDC_ERSST_v3b_SST.nc`.
2. Selected the Niño 3.4 region defined as 5°S–5°N and 170°W–120°W. In longitude, this corresponds to 190°E–240°E in the dataset.
3. Applied latitude-dependent area weights proportional to cos(latitude), then computed, for each month, the spatially weighted mean SST over the Niño 3.4 region.
4. Converted the time coordinate to monthly timestamps and extracted calendar months (1–12).
5. Calculated monthly climatology by averaging all January values together, all February values together, and so on over the entire record.
6. Subtracted the corresponding monthly climatology from each SST value to obtain a Niño 3.4 anomaly time series.

Results

- The monthly climatology shows only a modest seasonal cycle in the equatorial Pacific, with SSTs slightly warmer around boreal spring and early autumn, and slightly cooler in boreal winter.
- The anomaly time series exhibits large swings between warm and cold conditions, capturing El Niño (positive anomalies) and La Niña (negative anomalies) episodes.
- Typical anomalies range from about –2°C during strong La Niña events to +2–2.5°C during strong El Niño events, consistent with well-known ENSO behavior.
- Because climatology is removed, the mean of the anomaly series is close to zero, and the variability is dominated by interannual ENSO fluctuations rather than the seasonal cycle.

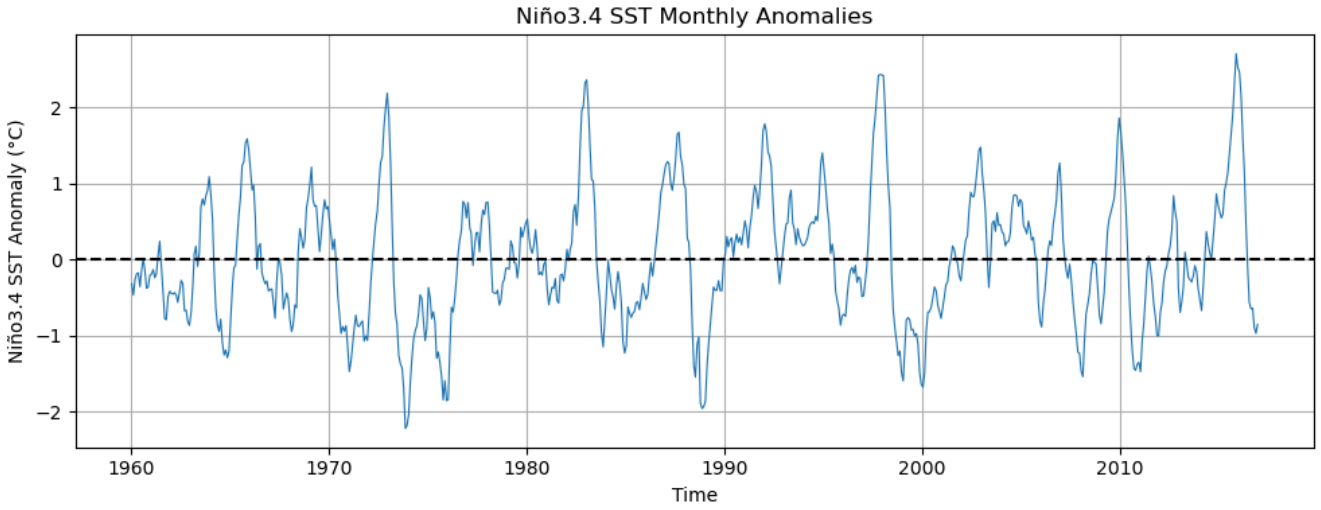

2.2 Visualization of Niño 3.4 anomalies

Method

1. Used the computed Niño 3.4 anomaly series and plotted monthly values as a continuous line from roughly the early 1960s to the 2010s.
2. Added a horizontal zero line to distinguish warm and cold phases relative to climatology.
3. Marked the +0.5°C and –0.5°C thresholds implicitly by visually comparing the anomaly amplitude to the y-axis scale (similar to the example figure).
4. Ensured the time axis and overall appearance qualitatively resemble the reference NOAA Niño 3.4 index plot.

Results

- The plot shows a sequence of warm and cold episodes matching the typical timing of historical ENSO events:
  - Large positive anomalies appear around the major El Niño events (e.g., early 1980s, late 1990s, mid-2010s), with peaks exceeding +2°C.
  - Pronounced negative anomalies occur during strong La Niña events, where SST anomalies dip below –1°C for extended periods.
- Several episodes stay above +0.5°C or below –0.5°C for at least five consecutive months, satisfying the operational definition of El Niño or La Niña conditions.
- Overall variability and patterns (frequency, amplitude, and timing) are qualitatively consistent with the NOAA Niño 3.4 index, confirming that the region selection, weighting, and climatology subtraction are implemented correctly.

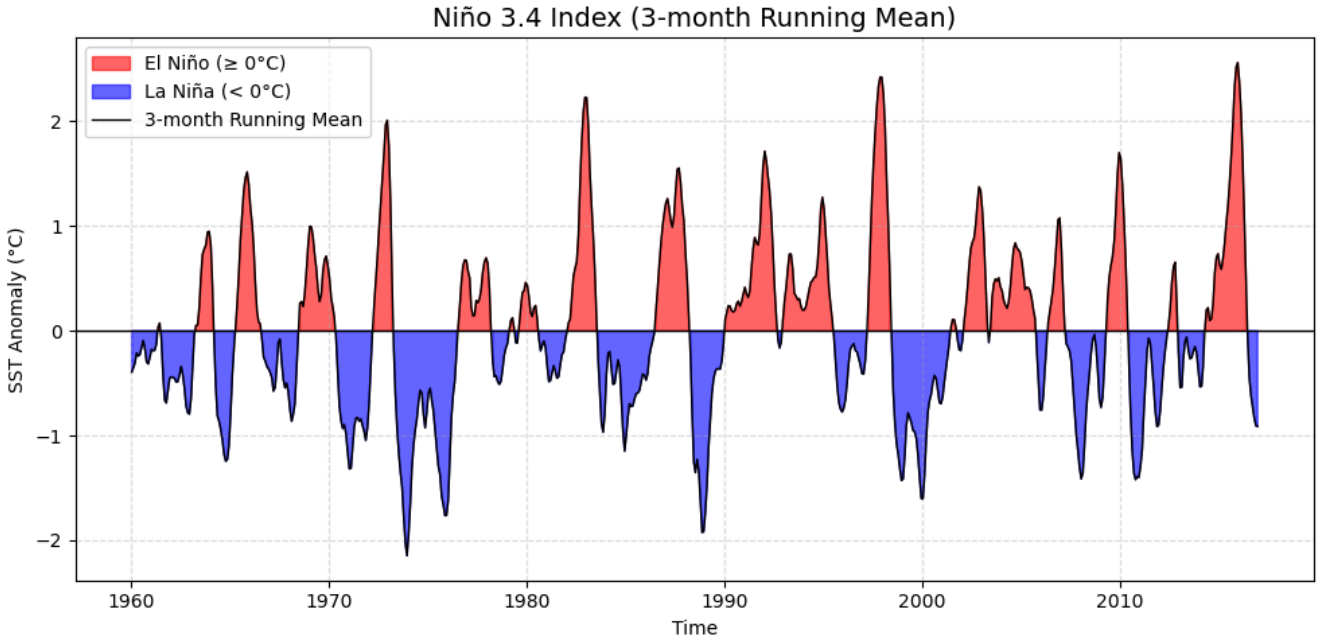

3. Exploring a GES DISC dataset: MERRA-2 BC column mass density

For this problem I explored the NASA GES DISC reanalysis product MERRA-2 aerosol diagnostics `https://disc.gsfc.nasa.gov/datasets/M2TMNXAER_5.12.4/summary?keywords=month`, using monthly mean two-dimensional fields (tavgM_2d_aer_Nx) from 1980-01 to 2024-01. The variable of interest is BCCMASS, the black carbon column mass density (kg m^{-2}).

3.1 Deseasonalized global BC time series

Method

- Downloaded monthly NetCDF files from 1980-01 to 2024-01 and combined them into a single xarray Dataset using `open_mfdataset`, matching files by coordinates.
- Selected the `BCCMASS` variable and treated non-finite values as missing.
- Computed a global mean time series using cos(latitude) as an area weight and averaging over longitude, so that polar regions are not over-represented.
- Grouped the global mean by calendar month to calculate a 12-month climatology (long-term average for each month).
- Subtracted the climatology from the global mean series, yielding a deseasonalized global BC anomaly time series.
- Plotted anomalies versus time with a horizontal zero line.

Results

- The deseasonalized global BC series fluctuates around zero with typical anomalies on the order of 10^{-7}–10^{-6} kg m^{-2}.
- Interannual variability is evident:
  - Some periods (e.g., late 1990s–early 2000s) show predominantly positive anomalies, likely associated with strong biomass burning and increasing fossil fuel emissions in developing regions.
  - Other periods (e.g., after certain pollution-control efforts) display more negative anomalies, suggesting a decrease in global BC burden.
- The underlying long-term pattern hints at a gradual rise in BC during the 1980s–2000s, followed by a possible leveling off or slight decline in more recent years, consistent with global air-quality regulations and technology changes.

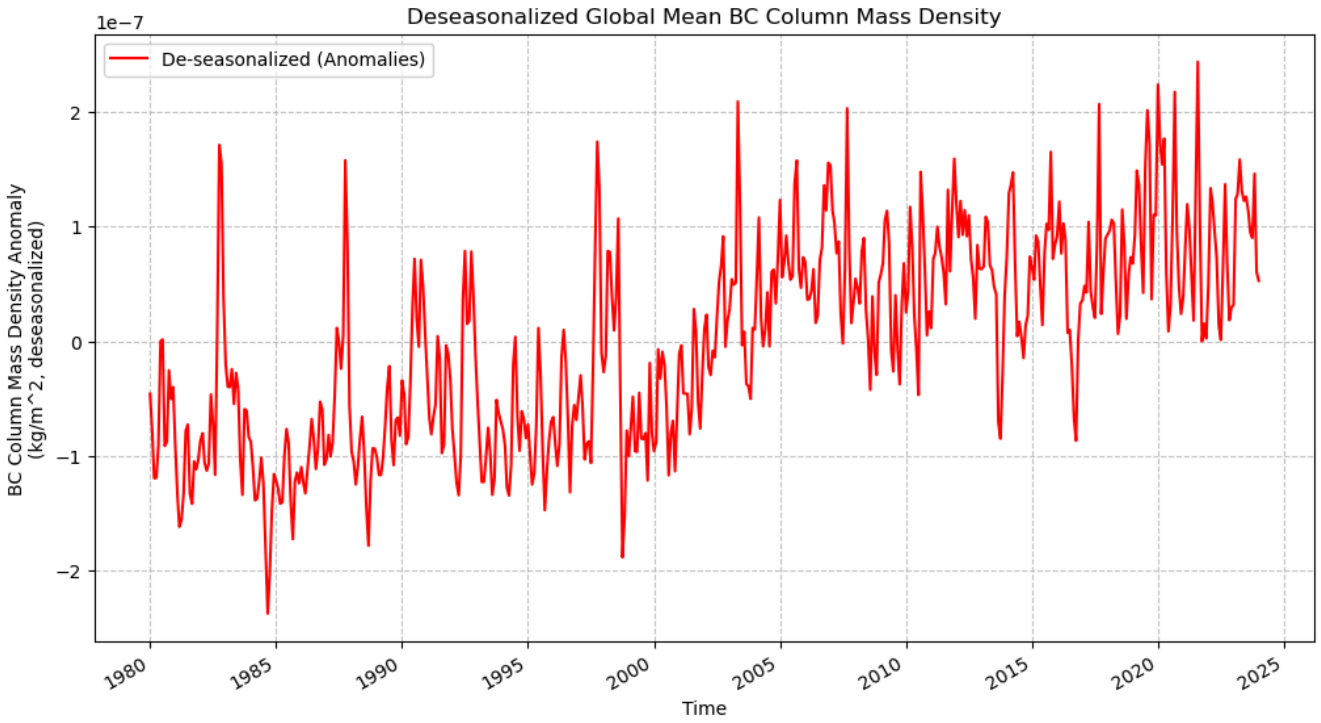

3.2 Additional plots from the BC dataset (five figures)

(1) Global mean BC original time series

Method

- Plotted the original global mean BCCMASS (before deseasonalization) as a function of time using the cos(latitude)-weighted global average.

Results

- The series shows a clear seasonal cycle, with repeating annual peaks and troughs superimposed on slower multi-decadal variations.
- Seasonal amplitude is relatively small compared with absolute values but still noticeable, reflecting seasonal changes in emissions (e.g., heating, biomass burning) and removal processes.
- Long-term variations agree qualitatively with the anomaly series: a gradual increase during the late 20th century followed by more mixed behavior afterwards.

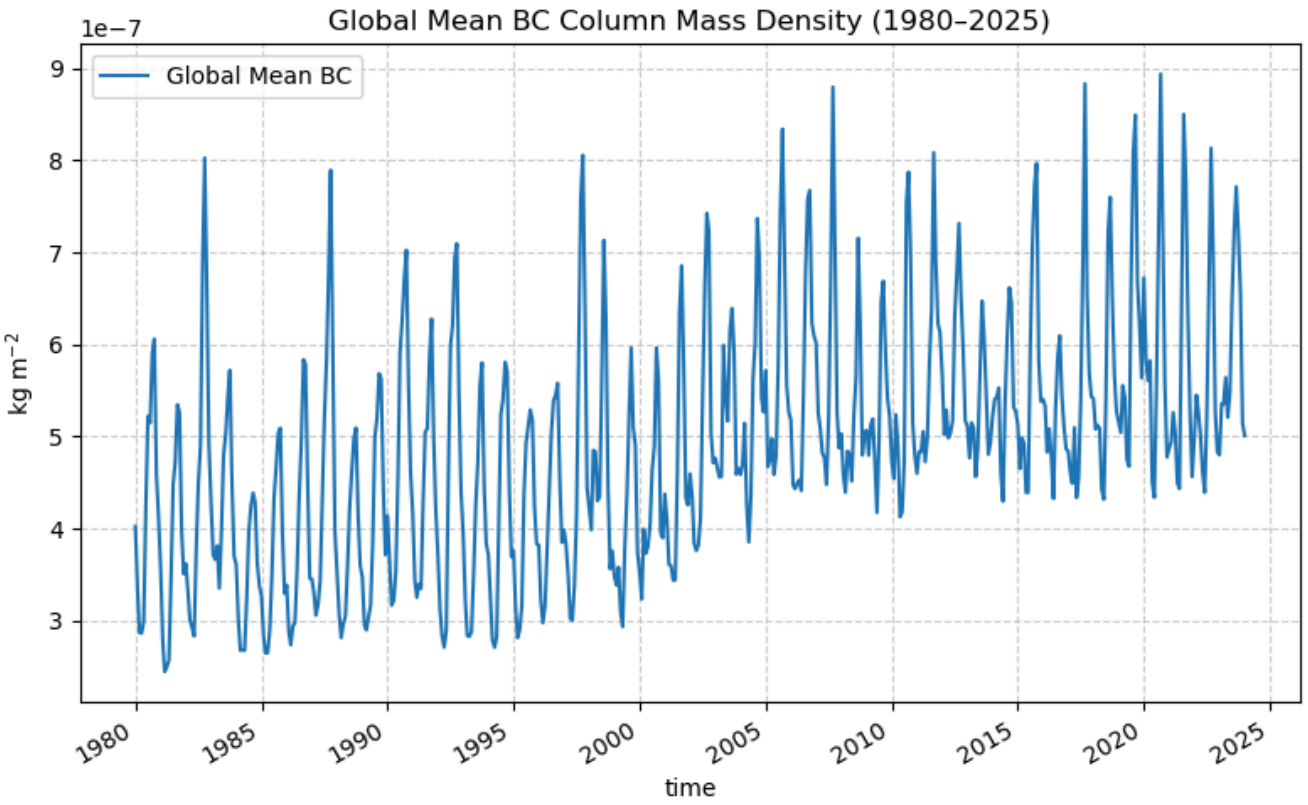

(2) Long-term mean spatial distribution (global BC map)

Method

- Averaged BCCMASS over the full time period to produce a single 2D spatial field (time mean).
- Displayed the field on a global Plate Carrée projection using Cartopy, with coastlines and labeled latitude/longitude ticks, and a colorbar in units of kg m^{-2}.

Results

- The map reveals strong spatial gradients in BC burden:
  - Highest values occur over South and East Asia (India, northern Indo-China, eastern China), consistent with dense population, coal use, and industrial emissions.
  - Elevated values also appear over central Africa, parts of South America, and Southeast Asia, corresponding to regions of persistent biomass burning.
  - Remote oceanic regions, polar areas, and sparsely populated land areas (e.g., central Pacific, Southern Ocean, interior Australia) show very low BC column mass.
- The pattern is physically reasonable and aligns with known global BC emission hotspots.

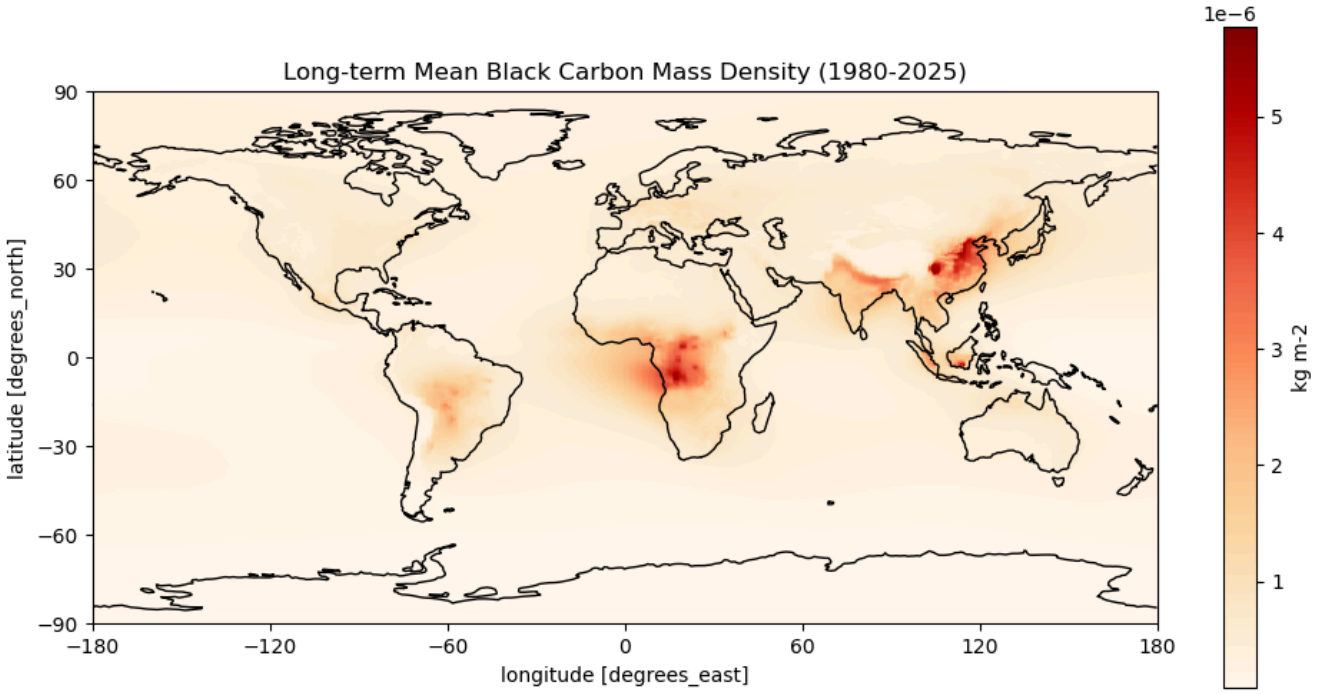

(3) Global seasonal cycle of BC

Method

- Using the global mean series, grouped data by calendar month and took the mean across years to obtain a 12-point seasonal cycle.
- Plotted month (1–12) on the x-axis and global mean BC on the y-axis, with markers and grid lines.

Results

- The seasonal cycle displays a single broad peak and trough per year:
  - Global BC tends to be higher during months associated with strong heating emissions in the Northern Hemisphere and peak biomass burning in the tropics.
  - Lower values typically occur during seasons with weaker combustion activity and enhanced wet scavenging.
- The amplitude of the seasonal cycle is modest relative to interannual variability but still evident, showing that BC emissions and removal processes are seasonally modulated at the global scale.

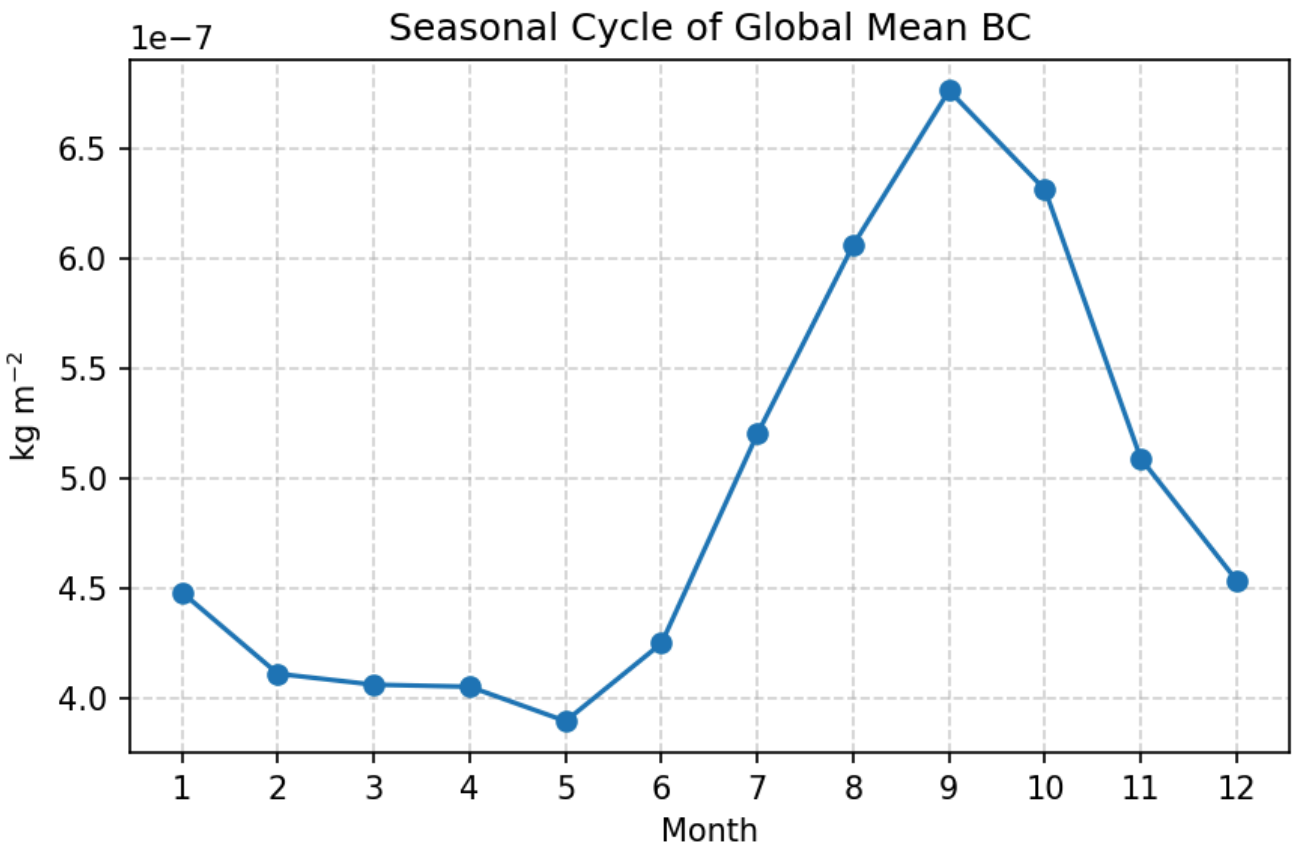

(4) Zonal mean profile (lat vs BC)

Method

- Computed a time-mean BCCMASS field, then averaged over longitude to obtain a zonal mean profile as a function of latitude.
- Plotted BC column density on the x-axis and latitude on the y-axis, with a horizontal line at the equator.

Results

- The zonal profile peaks in the Northern Hemisphere mid-latitudes (~20°N–40°N), where industrial and residential emissions are concentrated.
- There is a secondary enhancement around the northern tropics, influenced by both Asian emissions and long-range transport.
- The Southern Hemisphere generally exhibits much lower BC levels, with only modest bumps near regions of strong biomass burning (e.g., southern Africa, South America).
- The north–south asymmetry is consistent with known global patterns of fossil fuel usage and population distribution.

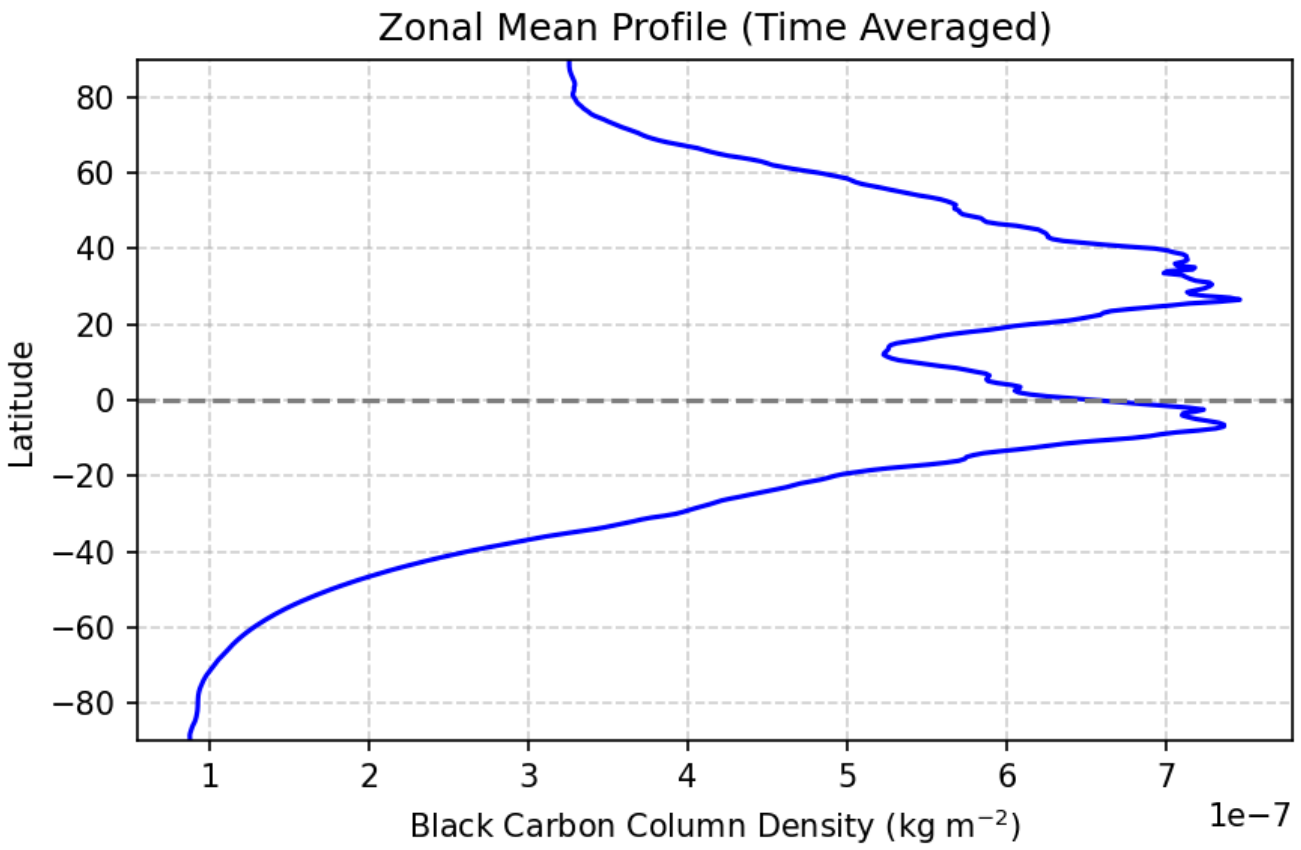

(5) Time–latitude Hovmöller diagram

Method

- Averaged BCCMASS over longitude at each time to form a time–latitude field.
- Plotted this as a Hovmöller diagram, with time on the x-axis, latitude on the y-axis, and color representing zonal-mean BC.

Results

- The diagram shows persistent bands of high BC at northern mid-latitudes, with gradual changes over decades:
  - Intensifying bands during the late 20th century suggest growing emissions from rapidly industrializing regions.
  - In more recent years, some latitudes exhibit stabilization or slight decreases, consistent with emission controls.
- Seasonal migration is also visible, with modest poleward-equatorward shifts of enhanced BC, especially in the Northern Hemisphere.
- The plot succinctly combines temporal and meridional information, making it easy to see both long-term trends and seasonal/interannual variations in the zonal mean.

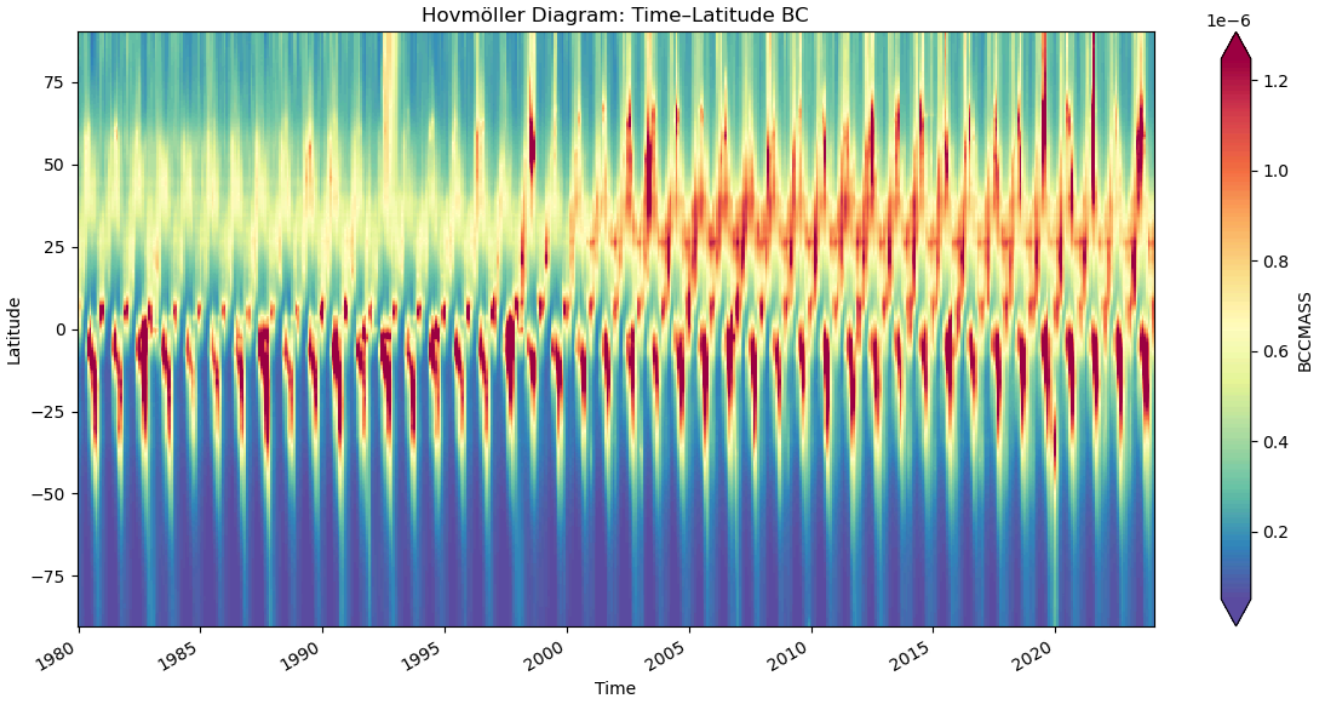

Collaboration

- I used ChatGPT to help me translate this report from Chinese to English.